

## HEAT TRANSFER IN A LOW LATITUDE FLAT-PLATE SOLAR COLLECTOR

by

**Chika Ogbonna Chima OKO\*** and **Stefen Ndubuisi NNAMCHI**

Department of Mechanical Engineering, Faculty of Engineering, University of Port Harcourt,  
Port Harcourt, Nigeria

Original scientific paper  
DOI: 10.2298/TSCI100419075O

*Study of rate of heat transfer in a flat-plate solar collector is the main subject of this paper. Measurements of collector and working fluid temperatures were carried out for one year covering the harmattan and rainy seasons in Port Harcourt, Nigeria, which is situated at the latitude of 4.858° N and longitude of 8.372° E. Energy balance equations for heat exchanger were employed to develop a mathematical model which relates the working fluid temperature with the vital collector geometric and physical design parameters. The exit fluid temperature was used to compute the rate of heat transfer to the working fluid and the efficiency of the transfer. The optimum fluid temperatures obtained for the harmattan, rainy and yearly (or combined) seasons were: 317.4, 314.9, and 316.2 K, respectively. The corresponding insolation utilized were: 83.23, 76.61, and 79.92 W/m<sup>2</sup>, respectively, with the corresponding mean collector efficiency of 0.190, 0.205, and 0.197, respectively. The working fluid flow rate, the collector length and the range of time that gave rise to maximum results were: 0.0093 kg/s, 2.0 m and 12:00-13:00 hour, respectively. There was good agreement between the computed and the measured working fluid temperatures. The results obtained are useful for the optimal design of the solar collector and its operations.*

Key words: *heat transfer, insolation, efficiency, low latitude, flat-plate solar collector, working fluid*

### Introduction

Solar energy absorbed by the solar collector could be used for several applications: heating and ventilation, drying operations, refrigeration, etc. [1]. In any form it is used, the heat has to be transferred from the absorbing device to utility device via the working fluid, which could be air or other working fluids [2]. The effectiveness of heat transfer could be measured by the thermal efficiency, which is a function of several parameters: the flow rate of the working fluid, the geometry of the collector, the optimum tilt angle, working fluid temperature, insolation utilizable, the overall heat transfer coefficient, the absorber plate temperature, and the ambient conditions [3].

Quantitative evaluation of the insolation utilizable from the collector to the dryer is necessary in order to determine the throughput of material to be dried from initial to final mois-

\* Corresponding author; e-mail: chimaoko@yahoo.com

ture content [4, 5]. In developing a model for the fluid temperature, the solar collector could be treated as a parallel flow heat exchanger with the collector plate temperature equivalent to that of hot fluid temperature. The mathematical model is based on the heat balance and heat transfer equations of the working fluid and of the collector, respectively [6]. This temperature will be used to determine the insolation utilized and the efficiency of the transfer.

Heat transfer either by conduction, convection or radiation is usually associated with resistance to the heat flux. The resistance to heat transfer is inversely proportional to the overall transfer coefficient, and a good heat transfer process must experience minimal resistance [7].

The flow rate of working fluid within the range of 0.0011-0.022 kg/s maximizes the heat transferred to the working fluid because of appreciable residence time of the working fluid in the collector [1, 8]. Increasing the surface area for the heat transfer increases the quantity of heat transferred to the working fluid [9]. The thermal efficiency of the thermal equipment (the flat-plate solar collector) ranges from 0.10-0.40 [10, 11] and it depends significantly on the convective heat transfer coefficient [12]. The thermal properties (the specific heat capacity and thermal conductivity) of the working fluid influence the ease of heat transfer. The length of the solar collector determines the residence time of the working fluid in the solar collector [1, 11, 13]. More heat is likely to be available between 12:00 and 13:00 hour, since maximum insolation lies within this interval; similarly, more insolation is obtained in the clear days (harmattan season) than in the cloudy days (rainy season) [14]. The inlet conditions of the working fluid influence the quantity of heat transferable and the optimum tilt angle enhances the amount of heat absorbable and transferable [1]. The latitude of a location partly determines the amount of heat absorbable and transferable [15, 16].

The critical parameters, which determine the amount of heat transferable, may limit the amount of solar heat transferred if not properly determined. These critical parameters are built into the mathematical model which describes the rate of heat transfer in the solar collector. Thus, this paper is concerned with developing a mathematical model, which can be used to predict the working fluid temperature, the rate of heat transfer to the working fluid and the efficiency of its transfer in a flat-plate solar collector.

### The governing equations

The rate of heat transfer in the flat-plate solar collector is modelled base on the assumption that heat transfer in the thermal equipment could be treated as a parallel flow heat exchanger with uniform collector plate temperature equivalent to that of the hot fluid. The rate of heat transfer,  $\dot{Q}_u$  [W] is given in [9] as:

$$\dot{Q}_u = U_L A_c \Delta t_m = \dot{m}_a c_{p,a} \Delta t \quad (1)$$

The rate of heat transfer per unit area of the collector,  $\dot{q}_u$  [ $\text{Wm}^{-2}$ ] is given as:

$$\dot{q}_u = \frac{\dot{Q}_u}{A_c} \quad (2)$$

where the logarithmic mean temperature difference is:

$$\Delta t_m = \frac{\Delta t_2 - \Delta t_1}{\ln \frac{\Delta t_2}{\Delta t_1}} \quad (3)$$

$\Delta t_1 = t_s - t_i$ ,  $\Delta t_2 = t_s - t_o$ , and  $\Delta t = t_o - t_i$ ;  $U_L$  [ $\text{Wm}^{-2}\text{K}^{-1}$ ],  $A_c$  [ $\text{m}^2$ ],  $t$  [ $^{\circ}\text{C}$ ],  $c_p$  [ $\text{kJkg}^{-1}\text{K}^{-1}$ ] and  $\dot{m}$  [ $\text{kg s}^{-1}$ ] are overall heat transfer coefficient, heat transfer area, temperature, and the specific heat capacity working fluid, and flow rate of the working fluid, respectively; the subscripts a, c, i, o, s, and u designate the working fluid (air), collector, inlet, outlet, absorber surface (or plate), and quantity utilized, respectively.

Rearranging eq. (1) gives:

$$\frac{U_L A_c}{\dot{m}_a c_{p,a}} = \ln \frac{t_s - t_o}{t_s - t_i} = -\ln \frac{(t_s - t_o) + (t_o - t_i)}{t_s - t_o} \quad (4)$$

Taking exponent of eq. (4) gives

$$\exp\left(-\frac{U_L A_c}{\dot{m}_a c_{p,a}}\right) = 1 + \frac{t_o - t_i}{t_s - t_i} \quad (5)$$

Further rearrangement of eq. (5) gives the expression for the exit fluid temperature,  $t_o$  [K]

$$t_o = t_i + (t_s - t_i) \left[1 - \exp\left(-\frac{U_L A_c}{\dot{m}_a c_{p,a}}\right)\right] \quad (6)$$

where

$$A_c = l_c w_c \quad (7)$$

$w_c$  [m],  $l_c$  [m] and  $\dot{q}_s$  [ $\text{Wm}^{-2}$ ] are the collector width, length and the insolation reaching the absorber plate, respectively.

Substituting eq. (7) into eq. (6) for  $w_c = 1.0$  gives:

$$t_o = t_i + (t_s - t_i) \exp\left(-\frac{l_c}{\frac{\dot{m}_a c_{p,a}}{U_L}}\right) \quad (8)$$

where the parameters  $\dot{m}_a$  [ $\text{kg s}^{-1}$ ], and  $U_L$  [ $\text{Wm}^{-2}\text{K}^{-1}$ ] are evaluated as in [2].

For maximum heat removal from the absorber surface (or plate), the flow factor,  $F''$  [-] is defined as:

$$F'' = \frac{F_R}{F'} = \frac{\dot{m}_a c_{p,a}}{A_c U_L F'} \left[1 - \exp\left(-\frac{A_c U_L F'}{\dot{m}_a c_{p,a}}\right)\right] \quad (9)$$

where  $F'$  [-] and  $F''$  [-] are the efficiency and heat removal factors, respectively.

As the number of heat-transfer units go to infinity ( $A_c U_L F' / \dot{m}_a c_{p,a} \rightarrow \infty$ ),  $F'' \rightarrow 1$ .

Thus

$$\dot{m}_a \approx \frac{A_c U_L F'}{c_{p,a}} \quad (10)$$

where

$$U_L = U_t + U_b \quad (11)$$

and  $U_b$  and  $U_t$  are the bottom and top overall heat-transfer coefficients, respectively:

$$U_t = \left[ \frac{1}{h_{s-c} + h_{r,s-c}} + \frac{1}{h_{c-sky} + h_{r,c-sky}} \right]^{-1} \quad (12)$$

and

$$U_b = \frac{1}{\frac{1}{h_{s-c}} + \frac{\delta_s}{k_s} + 2\frac{\delta_{pw}}{k_{pw}} + \frac{\delta_{rw}}{k_{rw}} + \frac{1}{h_{c-sky}}} \quad (13)$$

where  $h_{s-c}$  [ $\text{Wm}^{-2}\text{K}$ ] and  $h_{r,s-c}$  [ $\text{Wm}^{-2}\text{K}$ ] are the convective and radiative heat transfer coefficients between the absorber plate and the glass cover, respectively;  $h_{c-sky}$  [ $\text{Wm}^{-2}\text{K}^{-1}$ ] and  $h_{r,c-sky}$  [ $\text{Wm}^{-2}\text{K}^{-1}$ ] are the convective and radiative heat transfer coefficients between the glass cover and the sky, respectively;  $k_s$  [ $\text{Wm}^{-1}\text{K}^{-1}$ ] and  $\delta_s$  [m] are the thermal conductivity and the thickness of the collector materials, respectively, as shown in fig. 1(b). The expressions for the heat transfer coefficients are given as:

$$h_{c-sky} = 5.7 + 3.8v_{\text{wind}} \quad (14)$$

$$h_{r,c-sky} = \varepsilon_c \sigma (T_c^2 + T_{\text{sky}}^2) (T_c + T_{\text{sky}}) \quad (15)$$

where the sky temperature,  $T_{\text{sky}}$  [K] is:

$$T_{\text{sky}} = 0.0552T_{\text{amb}}^{1.5} \quad (16)$$

$$h_{r,s-c} = \frac{\sigma(T_s^2 + T_c^2)(T_s + T_c)}{\frac{1}{\varepsilon_s} + \frac{1}{\varepsilon_c} - 1} \quad (17)$$

$$h_{s-c} = \frac{\text{Nu}k_a}{D_H} \quad (18)$$

$$F' = \frac{1}{1 + \frac{h_{r,s-c}U_t}{h_{r,s-c}h_1 + h_{s-c}U_t + h_{s-c}h_{r,s-c} + h_1h_{s-c}}} \quad (19)$$

where

$$h_1 = \left( \frac{1}{U_t} - \frac{\delta_H}{k_H} - \frac{1}{h_{c-sky}} \right)^{-1}$$

The equivalent hydraulic diameter of the cross-section of the collector,  $D_H$  [m] is:

$$D_H = \frac{2\delta_H w_c}{\delta_H + w_c} \quad (20)$$

where  $\delta_H$  is the distance between the cover and the absorber plate.

The Nusselt number, Nu, for air in [2] is given as:

$$\text{Nu} = \left( 0.069 - 0.02 \frac{\phi^\circ}{90^\circ} \right) \sqrt[3]{\text{GrPr}} \text{Pr}^{0.074} \quad (21)$$

where  $\text{Gr} > 2 \cdot 10^5$  and  $0^\circ < \phi^\circ < 90^\circ$ ;  $\phi^\circ$  is the optimum tilt angle.

The Grashof, Gr, and Prandtl, Pr, numbers are defined as:

$$\text{Gr} = \frac{g \beta \Delta T D_H^3}{\nu_a^2} \quad (22)$$

$$\text{Pr} = \frac{c_{p,a} \mu_a}{k_a} \quad (23)$$

The collector efficiency,  $\eta_c$  [-], is given as:

$$\eta_c = \frac{q_u}{q_s} \quad (24)$$

where  $q_s$  [ $\text{Wm}^{-2}$ ] is the insolation reaching the absorber plate.

### Measurements

Drying equipment is made up of a flat-plate solar collector attached to a fixed-bed-drying chamber, fig. 1(a). The drying chamber is made up of two layers where the gains are placed. The collector is fitted with five thermocouples (Brannan K25616:0-160 °C; SPIR.1203:0-100 °C) at distance 0.0, 1.0, and 2.0 [m] along the collector. Two Taylor digital thermometers with humidity gauge (1422: 0-70 °C; 25-95 %) were used to measure the relative humidity at the inlet and exit of the collector. Thermocouple (AK688: 0-50 °C ) and Oxford digital multimeter (MY64) were used to measure the cover and plate temperatures, respectively. SILVS (0-360°) compass was used to align the collector along the South Pole. Measurements were taken on hourly basis starting from 9:00 to 16:00 hour for a period of one year. The measurements were carried out at Choba Campus of the Universality of Port Harcourt, Nigeria, which is suited at latitude of 4.858° N and longitude of 8.372° E.

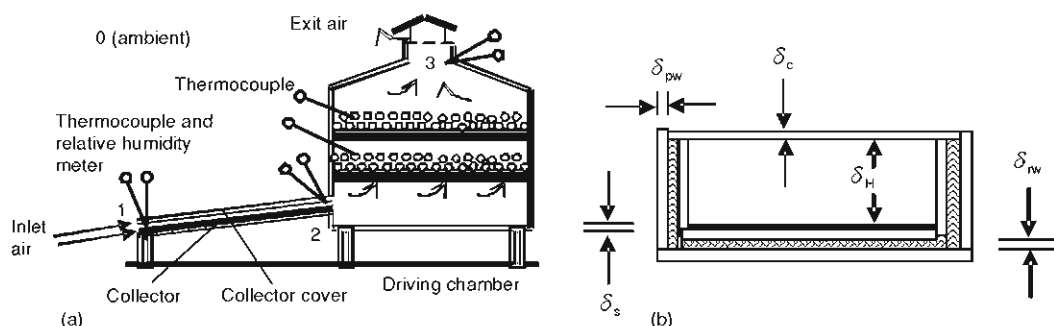


Figure 1. (a) Sketch of the flat-plate solar drying system, (b) cross-section of the collector

### Results and discussion

The following input parameters were specified:

- The collector effective surface area,  $A_c = 2.0 \text{ m}^2$ .
- The collector length,  $l_c = 2.0 \text{ m}$ .
- The collector width,  $w_c = 1.0 \text{ m}$ .
- The gravitational constant,  $g = 9.81 \text{ m/s}^2$ .
- Stefan-Boltzmann constant,  $\sigma = 5.6697 \cdot 10^{-8} \text{ W/m}^2\text{K}^4$ .
- The optimum slopes,  $\phi = 3.406^\circ$ ,  $3.750^\circ$ , and  $3.571^\circ$  for harmattan season, rainy season and yearly positioning, respectively.
- Emissivity of the absorber plate,  $\epsilon_s = 0.90$  and that of the glass cover,  $\epsilon_c = 0.88$ .
- Seasonal and yearly temperatures: Ambient ( $T_{amb}$ ), inlet fluid ( $T_i = T_{amb}$ ), cover glass ( $T_c$ ), absorber plate ( $T_s$ ) were tabulated in tab. 1.
- Seasonal and yearly wind speeds  $v_{wind}$  tabulated in tab. 1.

- The values for the thickness of glass cover ( $\delta_c$ ), plate ( $\delta_s$ ), plywood ( $\delta_{pw}$ ), rockwool ( $\delta_{rw}$ ) are tabulated in tab. 2.
- Thermal conductivities of glass cover ( $k_c$ ), plate ( $k_s$ ), plywood ( $k_{pw}$ ), rockwool ( $k_{rw}$ ) are tabulated in tab. 2.
- The thermal properties of working fluid (air): the specific heat capacity ( $c_p$ ), thermal conductivity ( $k$ ), viscosity ( $\mu$ ), and density ( $\rho$ ) are tabulated in tab. 3 as function of the working fluid temperature.

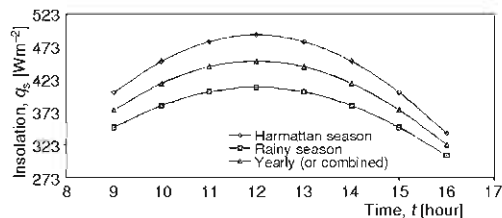
**Table 1. Seasonal and yearly input data for temperatures and wind velocity**

Harmattan season (November – April)					Rainy season (May – October)				Yearly			
Time	$T_i$ [K]	$T_c$ [K]	$T_s$ [K]	$V_{wind}$ [m/s]	$T_i$ [K]	$T_c$ [K]	$T_s$ [K]	$V_{wind}$ [m/s]	$T_i$ [K]	$T_c$ [K]	$T_s$ [K]	$V_{wind}$ [m/s]
9	296.9	308.8	320.7	1.02	295.4	305.8	316.7	0.96	296.2	307.3	318.7	0.99
10	298.7	311.6	327.4	1.08	297.1	309.7	322.9	1.01	297.9	310.7	325.1	1.04
11	299.1	313.3	332.3	1.15	297.7	312.8	328.6	1.07	298.4	313.0	330.4	1.11
12	301.6	318.0	336.2	1.19	299.8	315.7	333.3	1.10	300.7	316.8	334.8	1.15
13	303.2	318.8	337.4	1.23	301.6	316.9	334.2	1.15	302.4	317.9	335.8	1.19
14	301.0	317.4	332.5	1.12	299.3	315.8	329.6	1.04	300.1	316.6	331.0	1.08
15	300.0	315.4	331.0	1.08	298.8	314.1	328.6	1.00	299.4	314.7	329.8	1.04
16	299.0	313.7	325.1	1.02	298.2	312.6	324.8	0.94	298.6	313.1	324.9	0.98

**Table 2. Solid material input data**

Definition	Glass cover (c)	Plate (s)	Plywood (pw)	Rockwool (rw)
Thickness, $\delta$ [m]	0.004	0.001	0.0125	0.0175
Thermal conductivity, $k$ [W/mK]	0.761	204.26	0.140	0.042

The input data in tab. 1, the ambient, glass cover and absorber plate temperatures and the wind speed were obtained by measurements. Table 2 contains input data, the dimension and the thermal conductivity of the glass cover, absorber plate, plywood, and rockwool. Table 3 contains input data, the thermal properties of the working fluid (air) obtained from literature [17]. The discussion of the results will be based on seasonal and yearly data. The measurement periods were categorized into two: the harmattan season (comprising the following months: November, December, January, February, March, and April) and the rainy season (comprising: May, June, July, August, Septem-

**Figure 2. Seasonal and yearly insolation on the flat-plate solar collector**

ber, and October). The measurement periods were categorized into two: the harmattan season (comprising the following months: November, December, January, February, March, and April) and the rainy season (comprising: May, June, July, August, Septem-

ber, and October). The results in fig. 2 show that maximum insolation of 491.7, 451.4, and 411.1 W/m<sup>2</sup> occurred at noon for harmattan, rainy and yearly (or combined) seasons, respectively. Also, the solar radiation intensity for the computed harmattan result was greater than that of the yearly computed result, which was greater than that of the rainy season result.

**Table 3. Thermal properties of working fluid (air)**

Property	Symbol	Units	Equation
Specific heat capacity	$c_p$	KJ/kgK	$c_p = 1031.31 - 0.2047T + 0.00042T^2$ ; 280 < T < 400 [K]; R <sup>2</sup> = 1.0000
Thermal conductivity	$k$	W/mK	$k = 0.0121\exp(0.0026T)$ ; 280 < T < 400 [K]; R <sup>2</sup> = 0.9930
Viscosity	$\mu$	Ns/m <sup>2</sup>	$\mu = 1.0 \cdot 10^{-5}\exp(0.0021T)$ ; 300 < T < 400 [K]; R <sup>2</sup> = 1.0000
Density	$\rho$	kg/m <sup>3</sup>	$\rho = 2.1213 - 0.0031T$ ; 280 < T < 400 [K]; R <sup>2</sup> = 0.9825

The difference in magnitude of the solar radiation absorbed could be attributed to the sky conditions, which harmattan season has higher clearness index and higher relative sunshine than the rainy season in Port Harcourt zone, which is suited at latitude of 4.858° N.

Figure 3 shows the variation of seasonal and yearly fluid temperature at collector length of 2.0 m. The results show that maximum fluid temperature of 317.4, 314.9, and 316.2 K for harmattan, rainy and yearly (or combined) seasons, respectively, occurred between 12:00 to 13.00 hour which correspond to maximum insolation on the absorber plate (fig. 2). Also, Figure 3 shows that the magnitude of maximum insolation on the absorber plate for harmattan season was higher than that of rain season, which was higher than that of the combined seasons. This implies that drying of high moisture grains will be favoured in harmattan season than in the rainy season.

Besides, fig. 3 shows that there was good agreement between the measured and the computed fluid temperatures, which justifies that eq. (6) fairly predicts the fluid temperature along the solar collector.

Figure 4 shows the seasonal and yearly variation of fluid temperature with respect to flow rate for collector length of 2.0 m. The flow rate of the working fluid flow rate ranges from 0.0087 to 0.0097 kg/s was computed

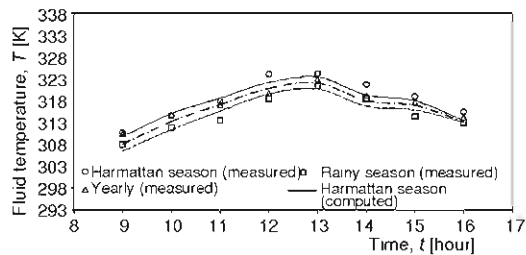


**Figure 3. Seasonal and yearly fluid temperature curve at the collector length of 2.0 m**

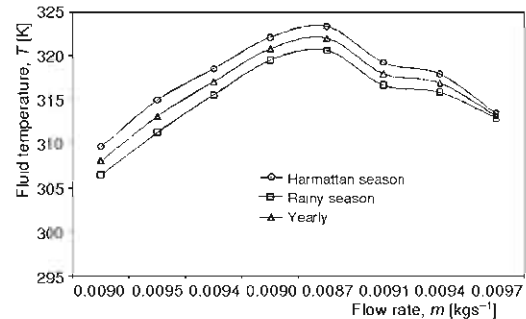


**Figure 4. Seasonal and yearly effect of air flowrate on the fluid temperature**

base on eq. (10). Besides, the results obtained were in agreement with the literature results [1, 8]. Maximum temperatures of 317.4, 314.9, and 316.2 K were attained at minimum fluid flow rate of 0.0094, 0.0092, and 0.0092 kg/s for harmattan, rainy and combined seasons, respectively. This is because the fluid had sufficient residence time in the solar collector than other flow rates observed. Regulating the flow rate of the working fluid under the natural convection will be onerous, requiring additional equipment and costs to be added to the solar collecting unit. However, more insolation will be transferred to the working fluid and its temperature raised above the recorded temperature.

The flow rate of fluids in the solar collector defined by eq. (10), was influenced by the

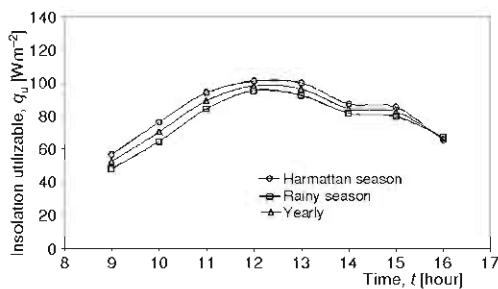


**Figure 5. Seasonal and yearly utilizable insolation at the collector length of 2.0 m**

which correspond to maximum absorbed insolation by the solar collector. Also, fig. 5 shows that harmattan season has higher value of maximum insolation utilized compared to those of rainy and combined seasons.

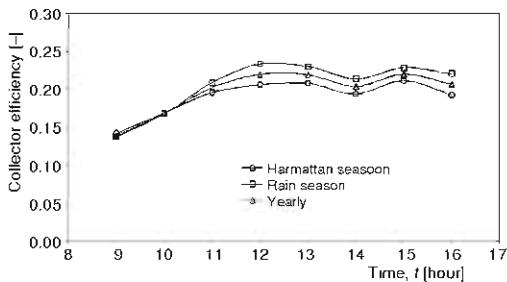


**Figure 6. Seasonal and yearly collector efficiency at the collector length of 2.0 m**

Also, fig. 5 shows that harmattan season has higher value of maximum insolation utilized compared to those of rainy and combined seasons. This implies that more insolation was available in harmattan season than in the rainy season.

Figure 6 shows the seasonal and yearly variation of collector efficiency with respect to time and for the collector length of 2.0 m for harmattan, rainy, and combined seasons, respectively. The results show that mean thermal efficiency of 0.1900, 0.2051, and 0.1974 occurred between 12:00 to 12.30 hour for harmattan, rainy and combined seasons, respectively. Also, fig. 6 shows that the collector efficiency was low at the sunrise (9:00) and at sunset (16:00) compared to hours of 10:00 to 15:00 hour because of high relative humidity of the former and low relative humidity of the latter. Moreover, the thermal efficiency obtained is within the range estimated in literatures [10, 11].

## Conclusions

The information found in the figs. 1-6 are useful in design optimization of the flat-plate solar collectors and for optimal operation of the solar collector.

Mathematical model for determining the temperature of the working fluid, the amount of insolation transferred from the absorber plate to the working fluid, the collector efficiency of



a flat-plate solar collector has been developed. There was good agreement between the computed and the measured fluid temperatures along the length of the flat-plate solar collector. Maximum insolation utilized was attained between 12:00 to 13:00 hour and at collector length of 2.0 m. Also, a flow rate of 0.0093 kg/s gave rise to highest insolation utilized in the solar collector. The collector efficiency of 0.190-0.205, shows that the solar collector was efficient and could meet the power requirement for thermal applications.

## References

- [1] Mohseni-Languri, E., *et al.*, An Exergy and Heat Study of a Solar Thermal Air Collector, *Thermal Science*, 13 (2009), 2, pp. 205-216
- [2] Duffie, J. A., Beckman, W. A., Solar Heat Thermal Processes, John Wiley and Sons Inc., New York, USA, 1974
- [3] Howell, J. R., Bannerot, R. B., Vliet, G. C., Solar-Thermal Energy Systems, McGraw-Hill, New York, USA, pp.122-158, 1982
- [4] Kuye, A., Oko, C. O. C., Nnamchi, S. N., Simulation of the Drying Characteristics of Ground Neem Seeds in a Fluidised Bed, *J. of Eng. and Tech.*, 2 (2007), 1, pp. 21-31
- [5] Pavlov, K. F., Romankov, P. G., Noskov, A. A., Examples and Problems to the Course of Unit Operations of Chemical Engineering, 1<sup>st</sup> ed., Mir Publishers, Moscow, 1979
- [6] Stoecker, W. F., Design of Thermal Systems, 3<sup>rd</sup> ed., McGraw-Hill, New York, USA, 1989
- [7] Kreith, F., Principles of Heat Transfer, 3<sup>rd</sup> ed., IEP-Dun-Donnelley Harper & Row Publishers, New York, USA, 1973
- [8] Soponronnarit, S., Solar Drying in Thailand, *Heat for Sustainable Development*, 11 (1995), 2, pp. 19-25, 1995
- [9] Oko, C. O. C., Introduction to Heat Transfer: An Algorithmic Approach, Pam Unique Publishing Coy., Port Harcourt, Nigeria, 2005
- [10] Zamfir, E., *et al.*, Simple and Accurate Method to Evaluate the tie-averaged performance of Flat-Plate Solar Collectors, *Heat Sources*, 18 (1996), 6, pp. 685-710
- [11] Ezekoye, B. A., Enebe, O. M., Development and Performance Evaluation of Modified Integrated Passive Solar Grain Dryer, *The Pacific Journal of Science and Technology*, 7 (2006), 2, pp. 185-190
- [12] Biondi, P., Licala, L., Farina, G., Performance Analysis of Solar Air Heaters of Conventional Design, *Solar Heat*, 41 (1988), 1, pp. 101-107
- [13] Khattab, N. M., Optimization of Hybrid Solar Dryer, *Heat Sources*, 18 (1996), 6, pp. 781-790
- [14] Ideriah, F. J. K., Suleman, S. O., Sky Condition at Ibadan during 1975-1980, *Solar Energy*, 43 (1989), 6, pp. 325-330
- [15] Qui, G., Riffat, S. B., Optimum Tilt Angle of Solar Collectors and its Impact on Performance, *International Journal of Ambient Energy*, 24 (2003), 1, pp. 13-20
- [16] Sodha, M. S., *et al.*, Solar Crop Drying, vol. I & II, CPR press, Boca Raton, Fla., USA, 1987
- [17] Welty, J. R., Wicks C. E., Wilson, R. E., Fundamentals of Momentum, Heat, and Mass Transfer, 2<sup>nd</sup> ed., John Wiley & Sons, New York, USA, 1976